

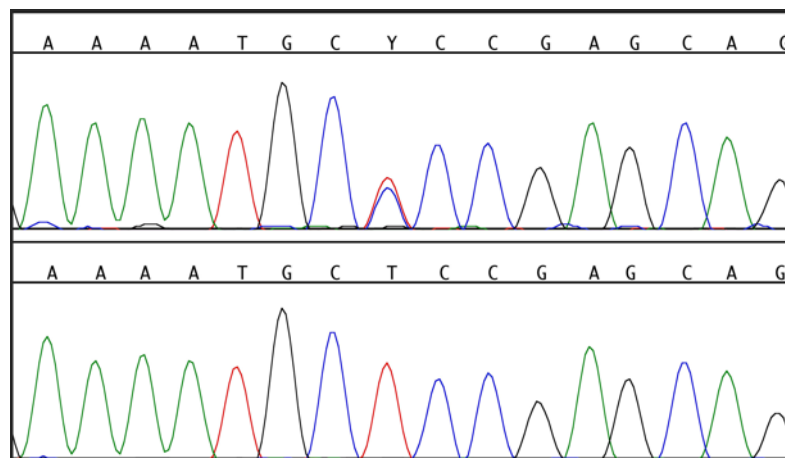
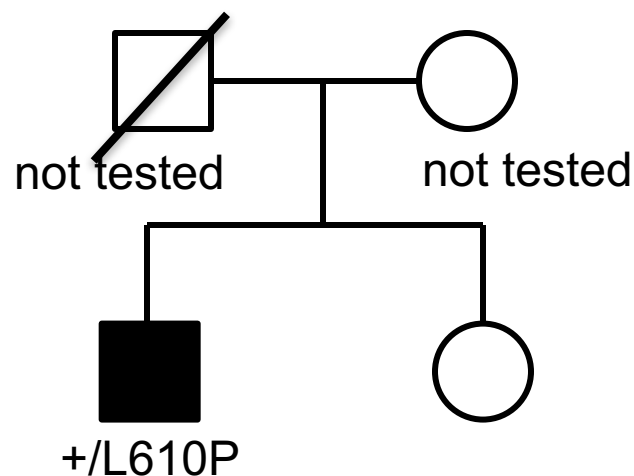
The American Journal of Human Genetics, Volume 103

## Supplemental Data

### Recurrent, Activating Variants in the Receptor Tyrosine Kinase *DDR2* Cause Warburg-Cinotti Syndrome

Linda Xu, Hanne Jensen, Jennifer J. Johnston, Emilio Di Maria, Katja Kloth, Ileana Cristea, Julie C. Sapp, Thomas N. Darling, Laryssa A. Hurn, Lisbeth Tranerbjærg, Elisa Cinotti, Christian Kubisch, Eyvind Rødahl, Ove Bruland, Leslie G. Biesecker, Gunnar Houge, and Cecilie Bredrup

**Figure S1: Pedigree of individual 1**

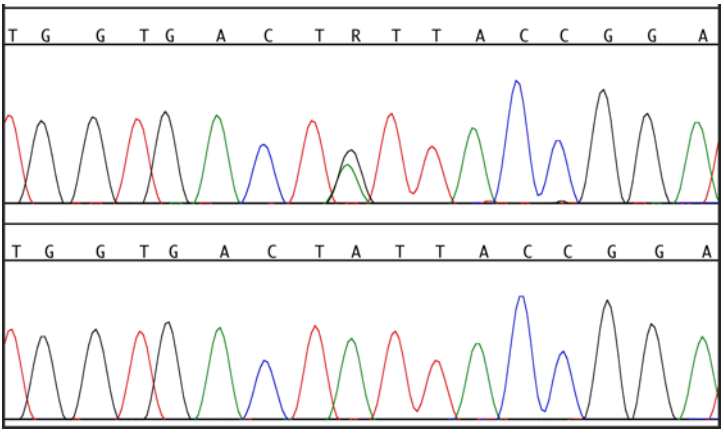
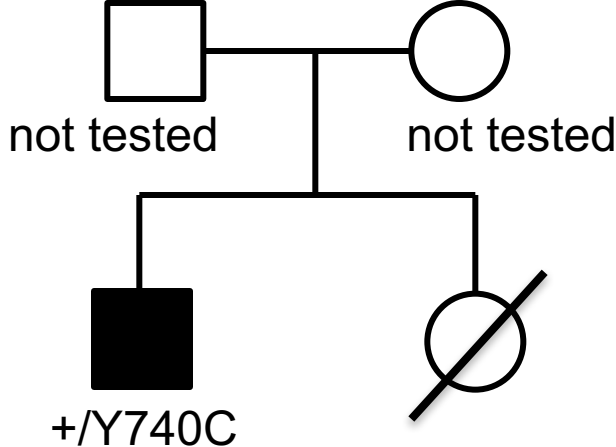


*DDR2*(NM\_001014796) c.1829T>C, p.(Leu610Pro)

Control DNA sample

*De novo* occurrence of the mutation could not be proven as DNA from the father was not available.

**Figure S2:** Pedigree of individual 2

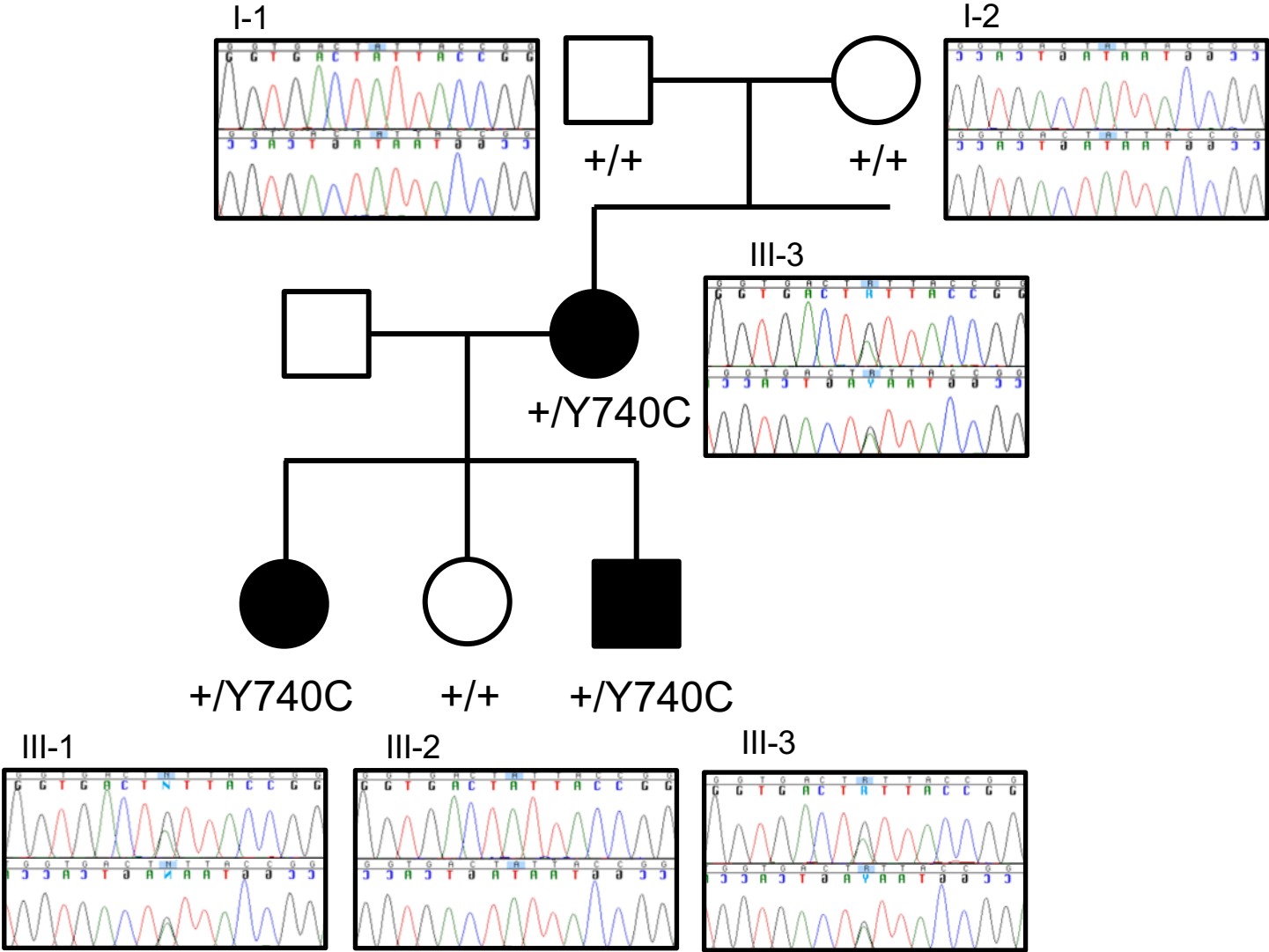


DDR2(NM\_001014796) c.2219A>G, p.(Tyr740Cys)

Control DNA sample

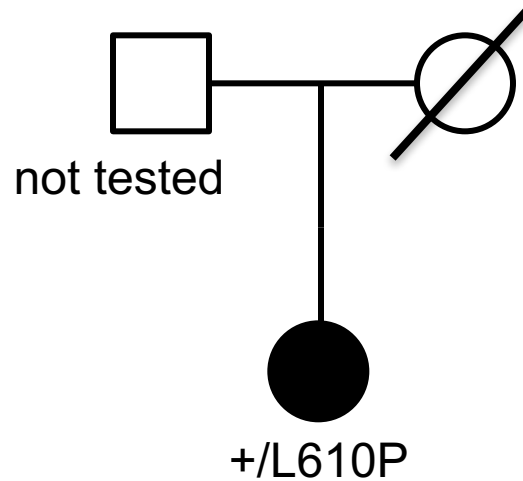
*De novo* occurrence of the mutation could not be proven as DNA from the parents was not available.

**Figure S3: Pedigree of individuals 3-5**



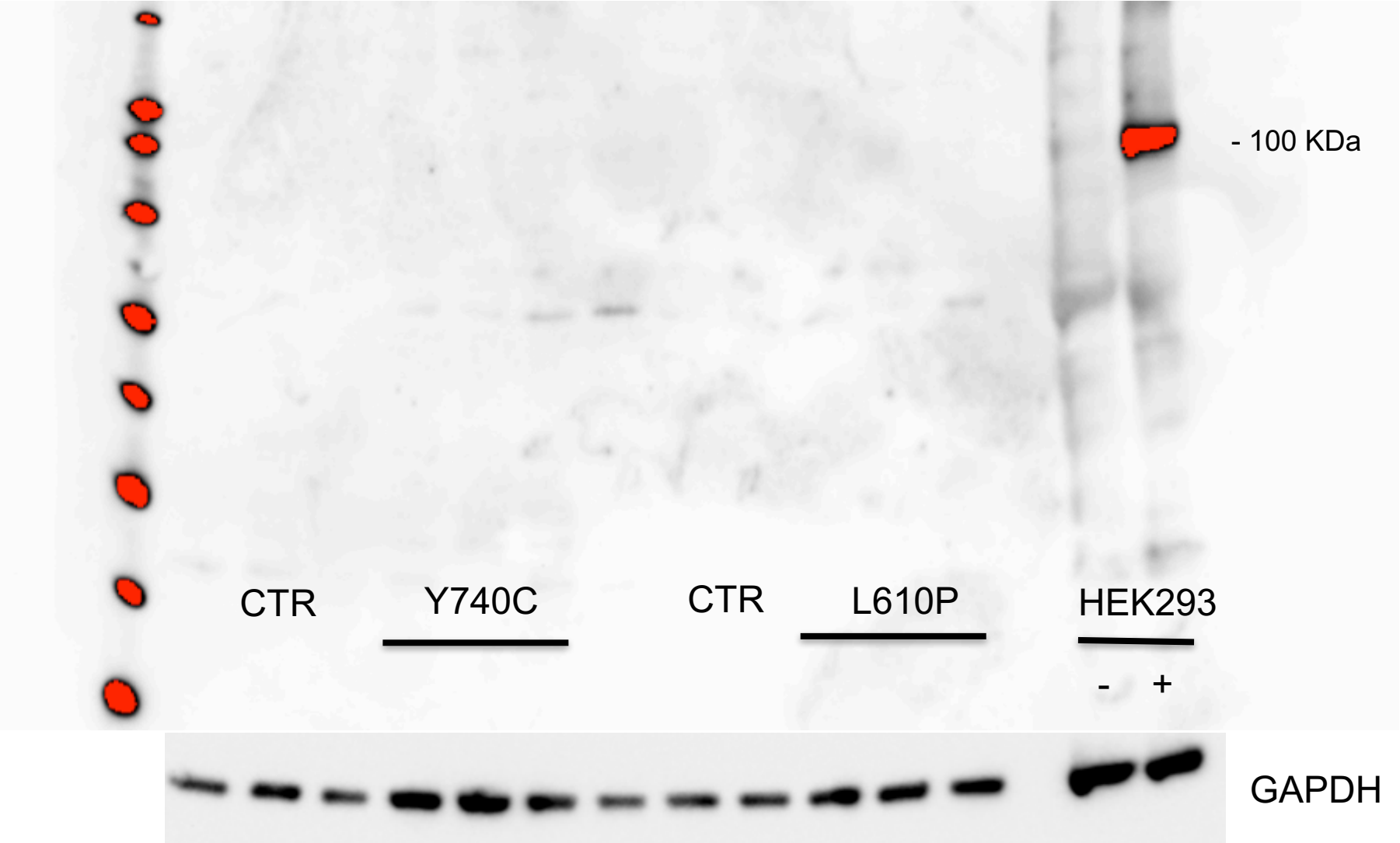
The mutation was proven *de novo* in II-2, and a biological relationship with II-1 and II-2 was verified. The electropherograms display the results of forward (top panels) and reverse (bottom panels) sequences.

**Figure S4:** Pedigree of individual 6



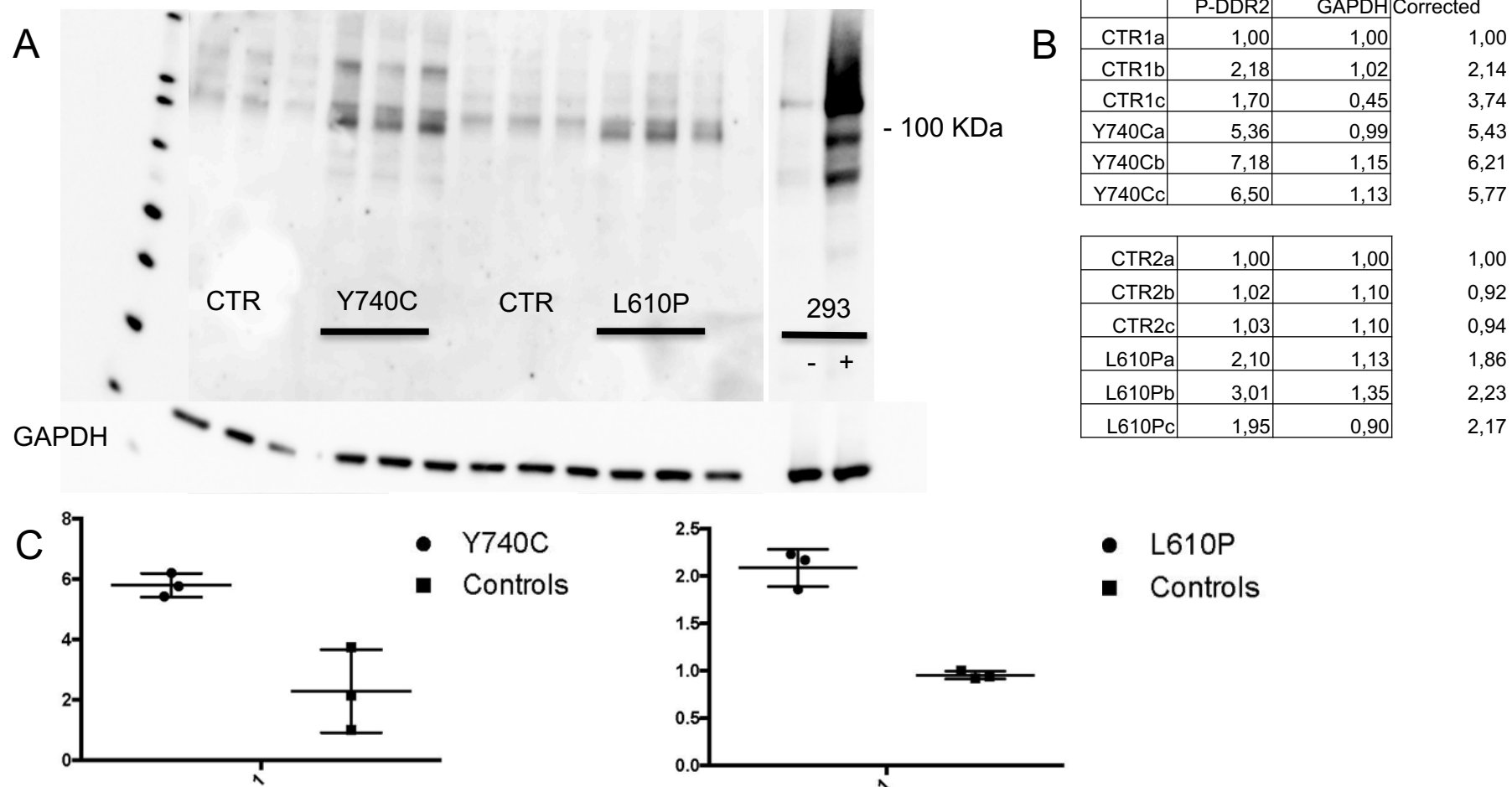
*De novo* occurrence of the mutation could not be proven as DNA from the parents was not examined.

**Figure S5: DDR2 immunoblot results**



Immunoblot analysis of fibroblasts harboring the p.(Leu610Pro) and the p.(Tyr740Cys) substitutions. DDR2 was undetectable in these cells. HEK 293 cells untransfected (-) or transfected (+) with DDR2 was used as control. Results from 3 parallel experiments.

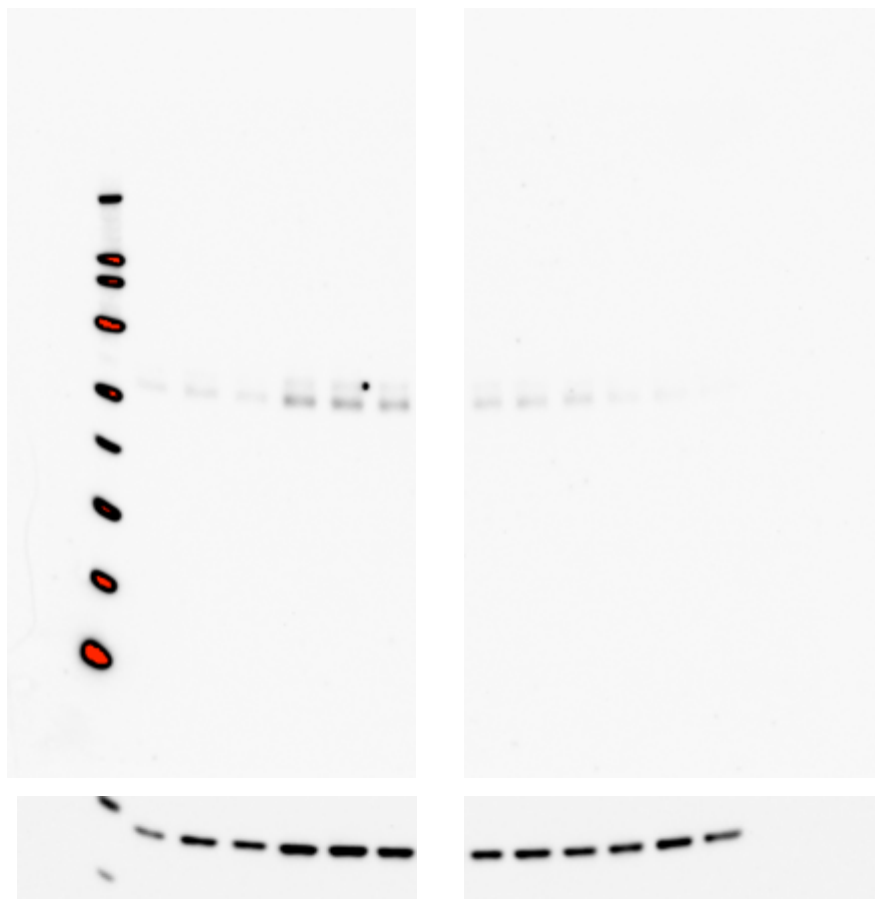
## Figure S6: Phospho-DDR2 immunoblot results



**A:** Immunoblot analysis of fibroblasts harboring the p.(Leu610Pro) and the p.(Tyr740Cys) substitutions. Increased levels of phospho-DDR2 (P-Tyr740) was detectable in patient fibroblast (Y740C and L610P). HEK 293 cells untransfected (-) or transfected (+) with DDR2 was used as control. Results from 3 parallel experiments.

**B and C:** results from relative quantifications. Measured values are approximately twice as high in fibroblasts from affected individuals. P=0.1 due to some variability in parallel experiments.

## Figure S7: Phospho-Tyr542-PTPN11/SHP-2 immunoblot results



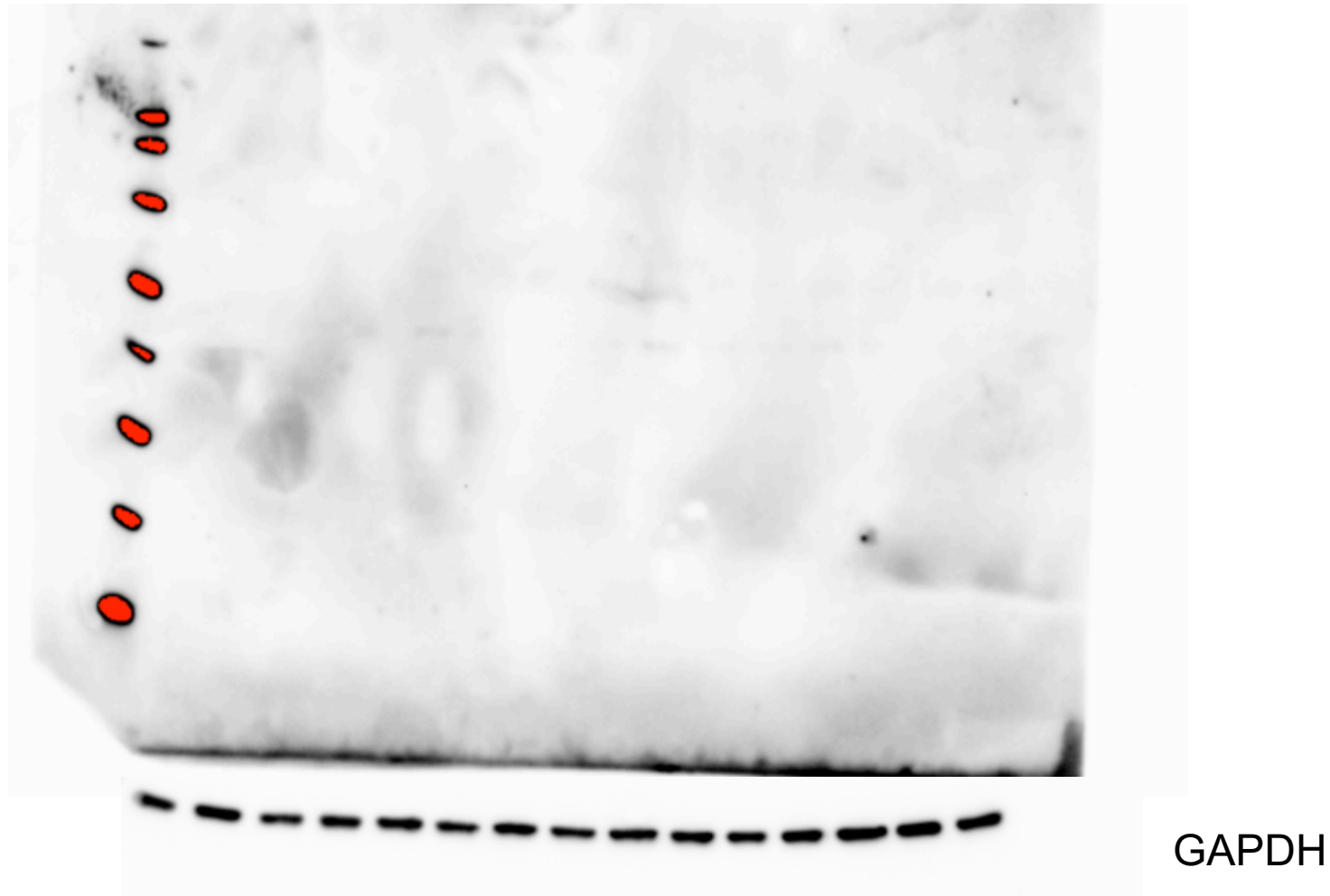
	P-Tyr542	GAPDH	Corrected
Ctr. A1	1,00	1,00	1,00
Ctr. A2	1,62	2,11	0,77
Ctr. A3	1,06	1,75	0,61
Y740C 1	7,01	3,54	1,98
Y740C 2	5,62	3,88	1,45
Y740C 3	4,74	3,06	1,55
L610P 1	2,62	1,98	1,32
L610P 2	2,25	2,39	0,94
L610 3	2,04	1,89	1,08
Ctr. B1	0,69	1,94	0,36
Ctr. B2	0,61	2,63	0,23
Ctr. B3	0,32	1,64	0,19

GAPDH

Immunoblot analysis of fibroblasts harboring the p.(Leu610Pro) and the p.(Tyr740Cys) substitutions. Slightly higher levels of phosphop-Tyr542-PTPN11 were found but this was not statistically significant. Results from 3 parallel experiments.

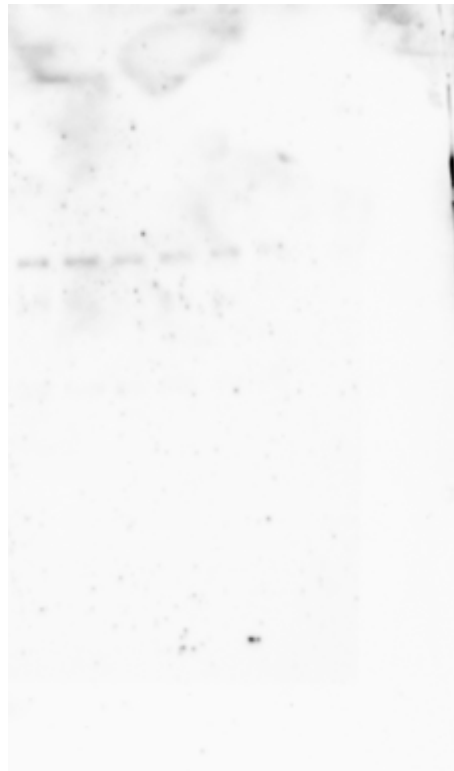
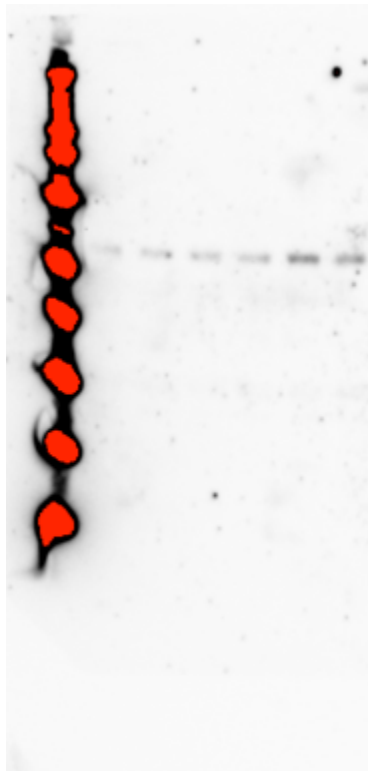


## Figure S8: Phospho-Tyr580-PTPN11 immunoblot results

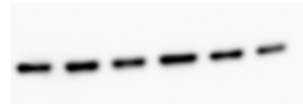
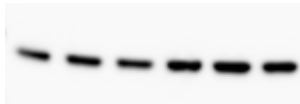


Immunoblot analysis of fibroblasts harboring the p.(Leu610Pro) and the p.(Tyr740Cys) substitutions. Phospho-Tyr580-PTPN11 was not detectable. Results from 3 parallel experiments.

## Figure S9: PTPN11/SHP-2 immunoblot results



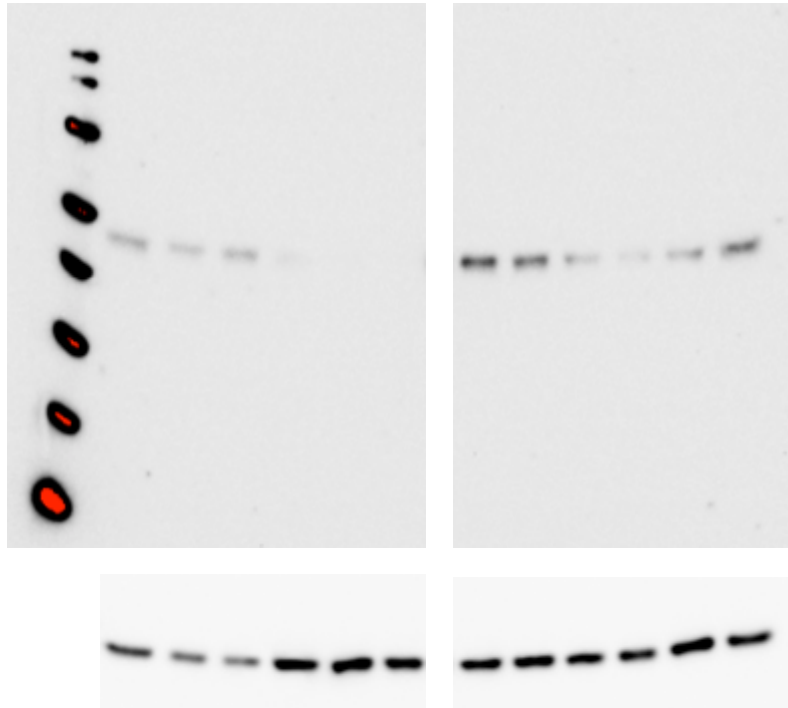
	PTPN11	GAPDH	Corrected
Ctr. A1	1,00	1,00	1,00
Ctr. A2	1,21	1,22	0,99
Ctr. A3	1,49	1,03	1,45
Y740C 1	1,58	1,64	0,97
Y740C 2	3,66	2,06	1,77
Y740C 3	3,75	1,62	2,32
L610P 1	1,21	1,19	1,02
L610P 2	1,72	1,33	1,29
L610 3	1,09	0,99	1,10
Ctr. B1	0,93	1,38	0,67
Ctr. B2	0,86	1,06	0,82
Ctr. B3	0,55	0,68	0,81



GAPDH

Immunoblot analysis of fibroblasts harboring the p.(Leu610Pro) and the p.(Tyr740Cys) substitutions. Slightly higher levels of PTPN11 were found but were not considered significant. Results from 3 parallel experiments.

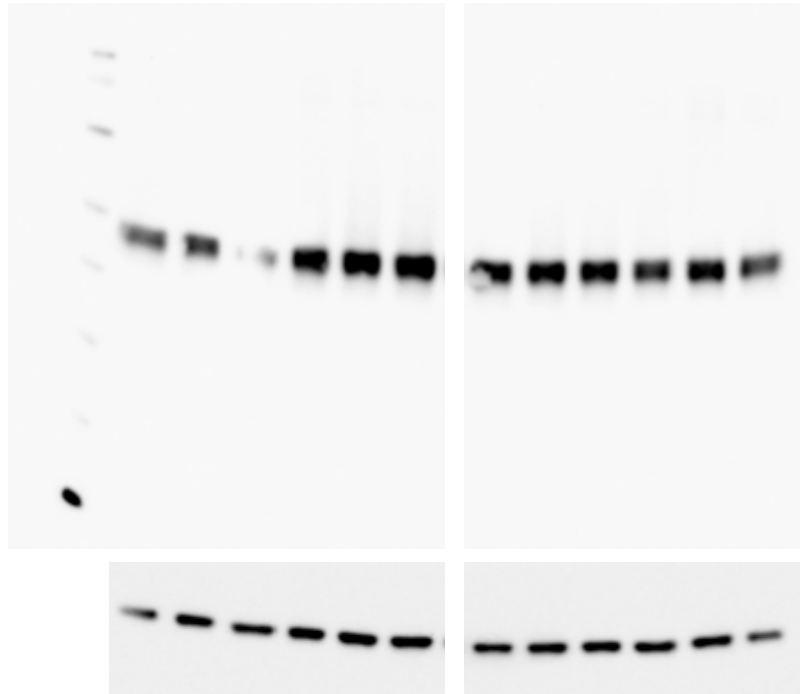
## Figure S10: Phospho-AKT immunoblot results



	P-AKT.	GAPDH.	Corrected
Ctr. A1	1,00	1,00	1,00
Ctr. A2	0,45	0,63	0,72
Ctr. A3	0,66	0,56	1,18
Y740C 1	0,17	1,83	0,09
Y740C 2	0,06	2,03	0,03
Y740C 3	0,07	1,44	0,05
L610P 1	2,17	1,44	1,51
L610P 2	1,61	1,58	1,02
L610 3	0,56	1,19	0,47
Ctr. B1	0,25	1,08	0,23
Ctr. B2	0,75	2,03	0,37
Ctr. B3	1,68	1,37	1,22

Immunoblot analysis of fibroblasts harboring the p.(Leu610Pro) and the p.(Tyr740Cys) substitutions. Slightly higher levels of phospho-AKT were found cells with the p.(Leu610Pro) substitution but this was not considered significant. Results from 3 parallel experiments.

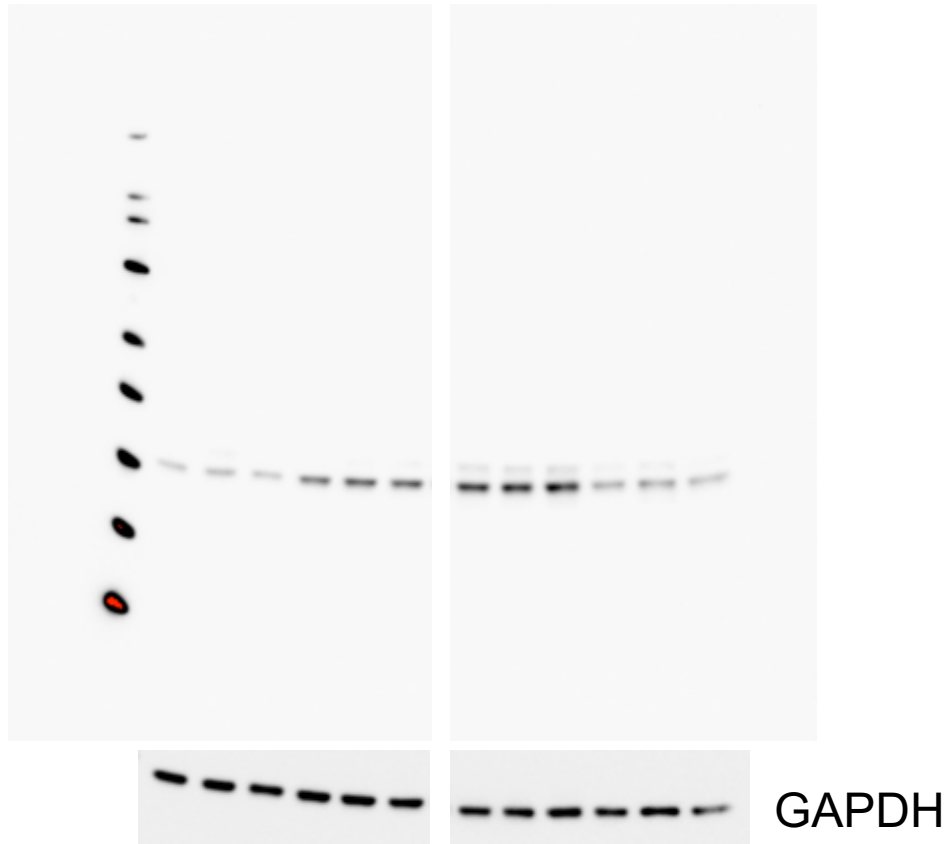
## Figure S11: AKT immunoblot results



	AKT	GAPDH	Corrected
Ctr. A1	1,00	1,00	1,00
Ctr. A2	1,02	1,84	0,56
Ctr. A3	0,26	1,65	0,16
Y740C 1	1,67	2,11	0,79
Y740C 2	2,12	2,35	0,90
Y740C 3	2,31	2,50	0,92
L610P 1	1,46	1,69	0,86
L610P 2	1,73	1,92	0,90
L610 3	1,66	1,89	0,88
Ctr. B1	1,30	1,86	0,70
Ctr. B2	1,57	1,91	0,82
Ctr. B3	1,19	1,04	1,14

Immunoblot analysis of fibroblasts harboring the p.(Leu610Pro) and the p.(Tyr740Cys) substitutions. Similar levels of AKT were present. Results from 3 parallel experiments.

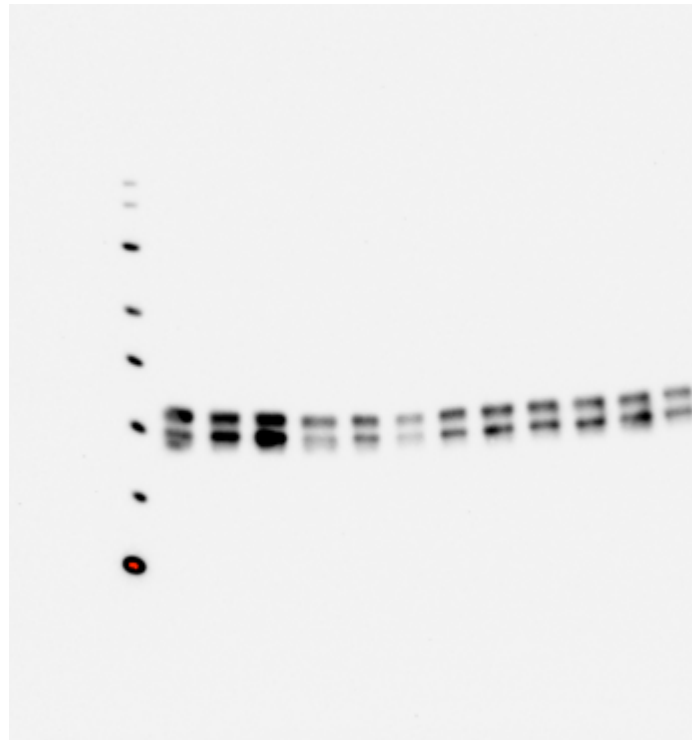
## Figure S12: Phospho-MAPK3/ERK1 immunoblot results



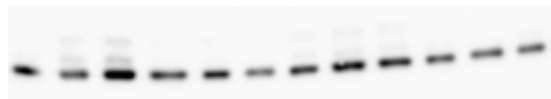
	P-ERK.	GAPDH	Corrected
Ctr. A1	1,00	1,00	1,00
Ctr. A2	1,28	1,00	1,28
Ctr. A3	1,01	0,86	1,17
Y740C 1	3,14	1,09	2,89
Y740C 2	3,94	1,05	3,74
Y740C 3	3,82	0,90	4,24
L610P 1	5,26	0,71	7,43
L610P 2	5,56	0,73	7,63
L610 3	6,23	0,90	6,93
Ctr. B1	2,10	0,67	3,12
Ctr. B2	2,57	0,92	2,79
Ctr. B3	1,78	0,50	3,53

Immunoblot analysis of fibroblasts harboring the p.(Leu610Pro) and the p.(Tyr740Cys) substitutions. Higher levels of phospho-MAPK3/ERK1 were found but were not reproduced in follow-up experiments as shown in Figure S14. Results from 3 parallel experiments.

## Figure S13: MAPK3/ERK1 immunoblot results



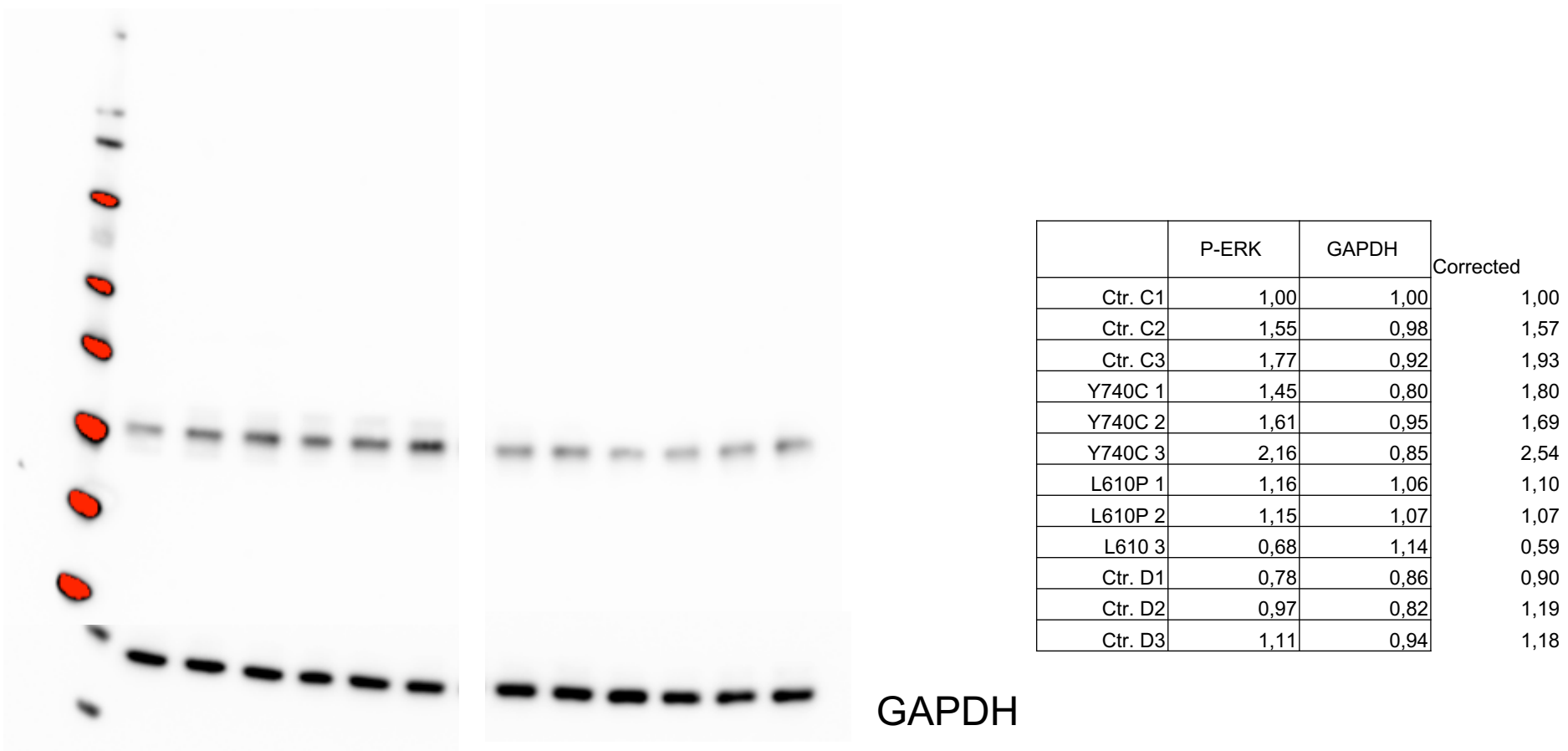
	ERK	GAPDH	Corrected
Ctr. A1	1,95	0,93	2,10
Ctr. A2	2,13	0,93	2,28
Ctr. A3	3,35	1,83	1,83
Y740C 1	1,00	1,00	1,00
Y740C 2	0,97	0,88	1,10
Y740C 3	0,44	0,64	0,69
L610P 1	1,02	0,86	1,18
L610P 2	1,43	1,24	1,15
L610P 3	1,32	1,06	1,24
Ctr. B1	1,35	0,74	1,82
Ctr. B2	1,55	0,77	2,01
Ctr. B3	0,85	0,66	1,29



GAPDH

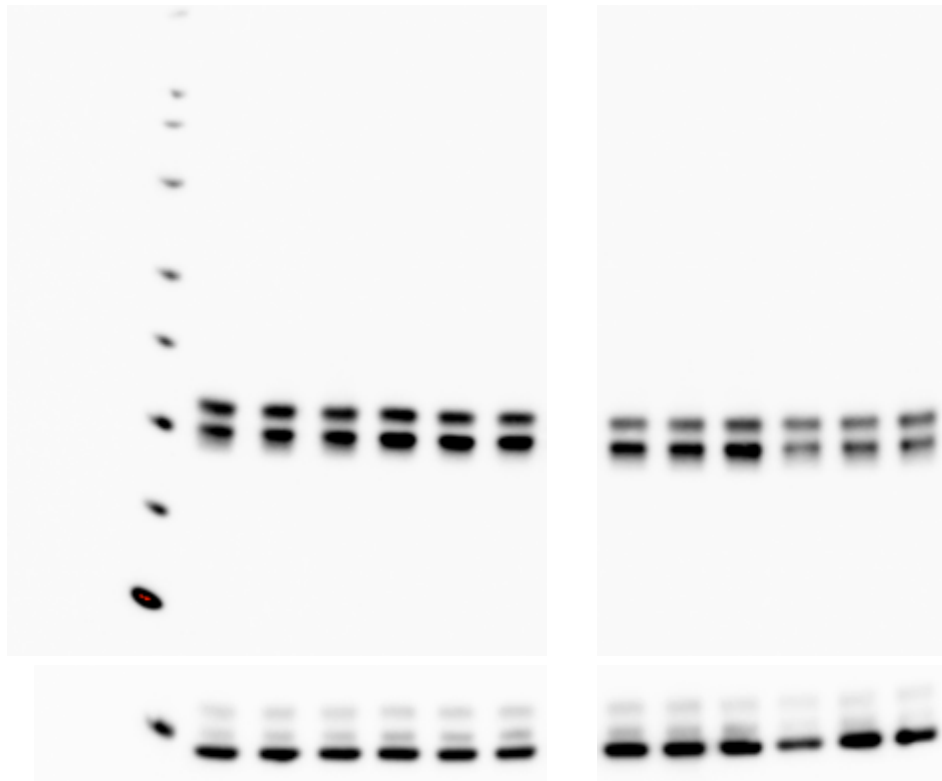
Immunoblot analysis of fibroblasts harboring the p.(Leu610Pro) and the p.(Tyr740Cys) substitutions. Similar levels of MAPK3/ERK1 was present. Results from 3 parallel experiments.

**Figure S14:** Phospho-MAPK3/ERK1 immunoblot results



Immunoblot analysis of fibroblasts harboring the p.(Leu610Pro) and the p.(Tyr740Cys) substitutions. Due to the finding higher levels of phospho-MAPK3/ERK1 shown in Figure S12 this was reproduced. In this experiment slightly higher levels of phospho-ERK were found in cells with the p.(Tyr740Cys) substitution but were not considered significant. Results from 3 parallel experiments.

## Figure S15: MAPK3/ERK1 immunoblot results

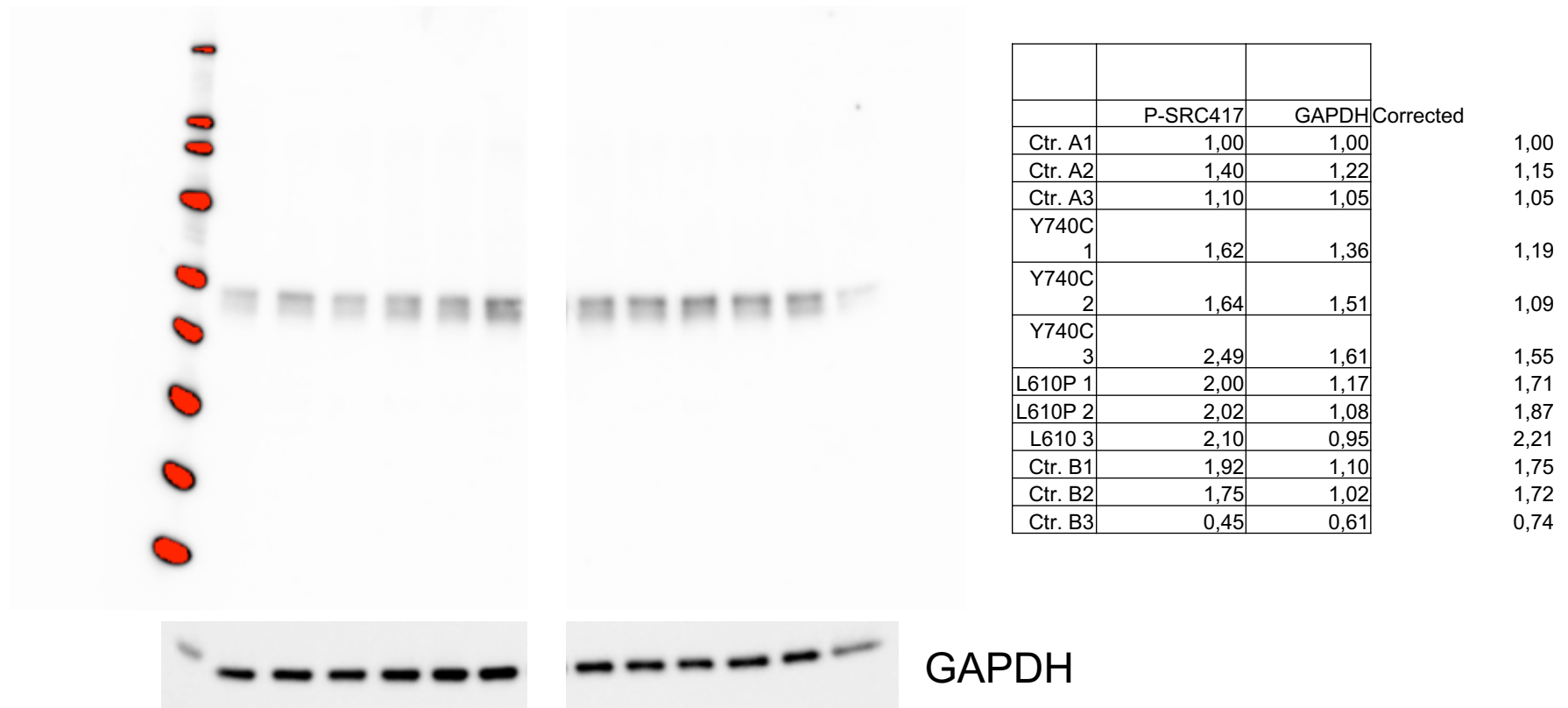


	GAPDH	ERK	Corrected
Ctr. C1	1,00	1,00	1,00
Ctr. C2	1,02	1,03	1,01
Ctr. C3	0,96	1,08	1,13
Y740C 1	1,04	1,31	1,26
Y740C 2	0,97	1,19	1,23
Y740C 3	0,93	1,13	1,21
L610P 1	1,45	0,89	0,61
L610P 2	1,45	0,93	0,64
L610 3	1,43	1,15	0,80
Ctr. D1	0,75	0,66	0,87
Ctr. D2	1,54	0,76	0,49
Ctr. D3	1,09	0,74	0,68

Immunoblot analysis of fibroblasts harboring the p.(Leu610Pro) and the p.(Tyr740Cys) substitutions. Similar levels of ERK was present. Results from 3 parallel experiments.

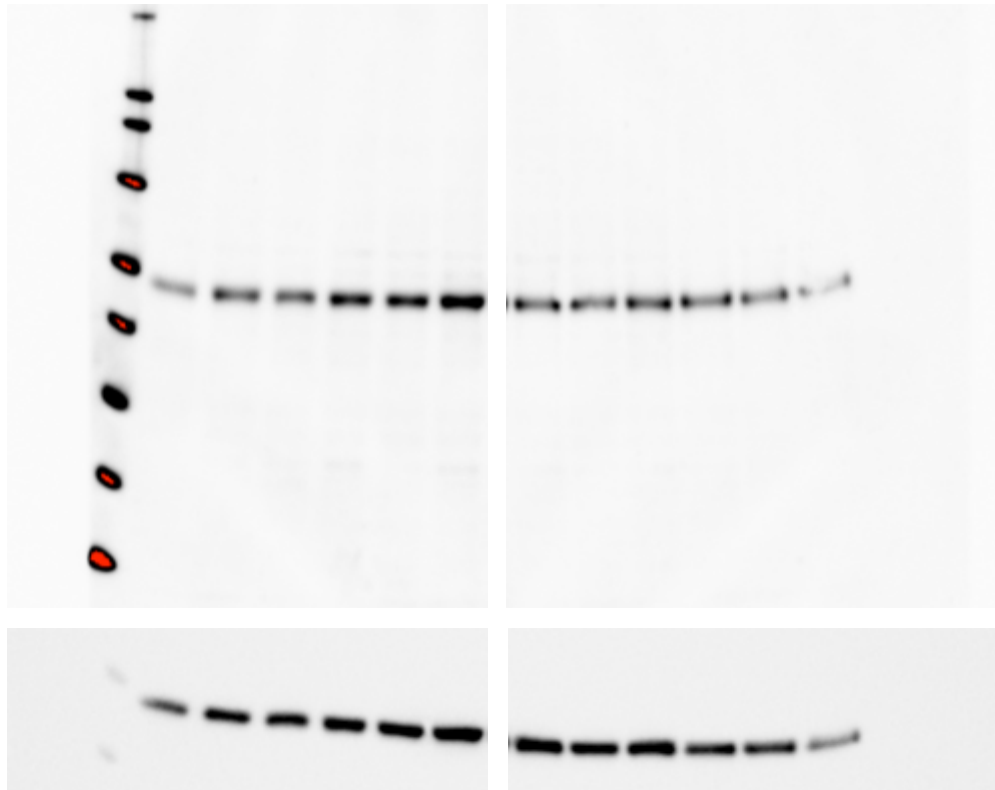


## Figure S16: Phospho-Tyr416-SRC immunoblot results



Immunoblot analysis of fibroblasts harboring the p.(Leu610Pro) and the p.(Tyr740Cys) substitutions. Similar levels of phospho-Tyr416-SRC were present. Results from 3 parallel experiments.

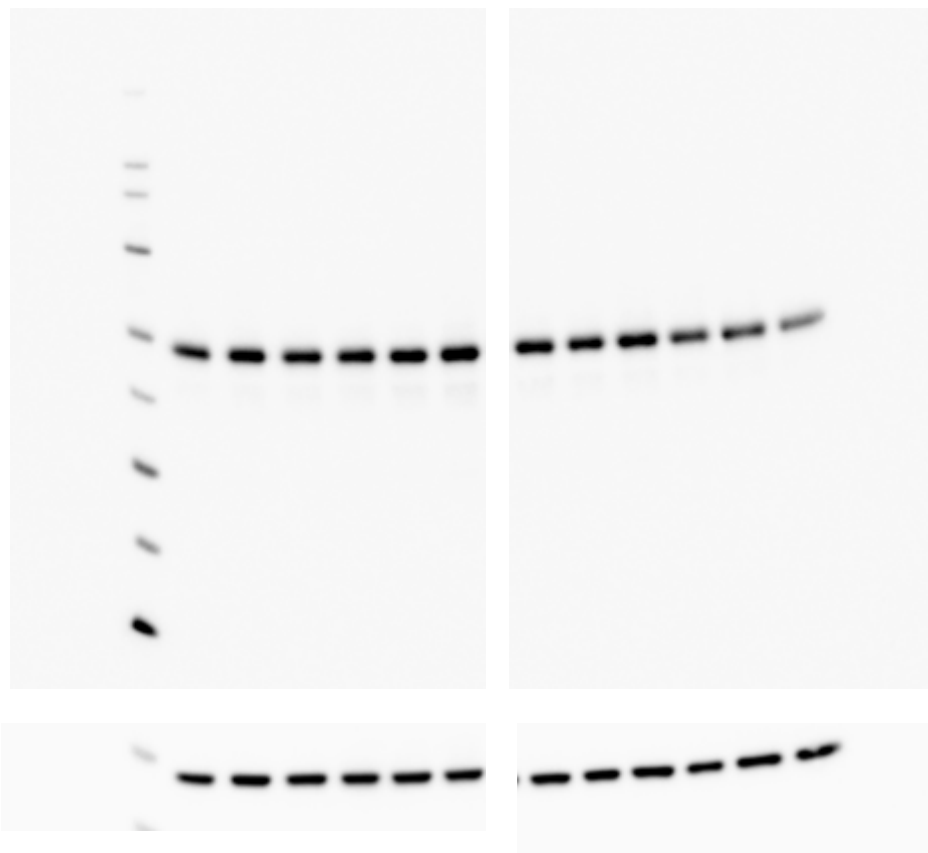
## Figure S17: Tyr416-SRC immunoblot results



	SRC416	GAPDH	Corrected
Ctrl. A1	1,00	1,00	1,00
Ctrl. A2	1,73	1,55	1,11
Ctrl. A3	1,49	1,41	1,06
Y740C 1	2,16	1,73	1,25
Y740C 2	2,17	1,98	1,10
Y740C 3	3,20	2,60	1,23
L610P 1	1,77	2,28	0,92
L610P 2	1,51	1,83	0,82
L610 3	1,94	2,04	0,95
Ctrl. B1	1,76	1,49	1,18
Ctrl. B2	1,40	1,41	0,99
Ctrl. B3	0,68	0,81	0,84

Immunoblot analysis of fibroblasts harboring the p.(Leu610Pro) and the p.(Tyr740Cys) substitutions. Similar levels of Tyr416-SRC was present. Results from 3 parallel experiments.

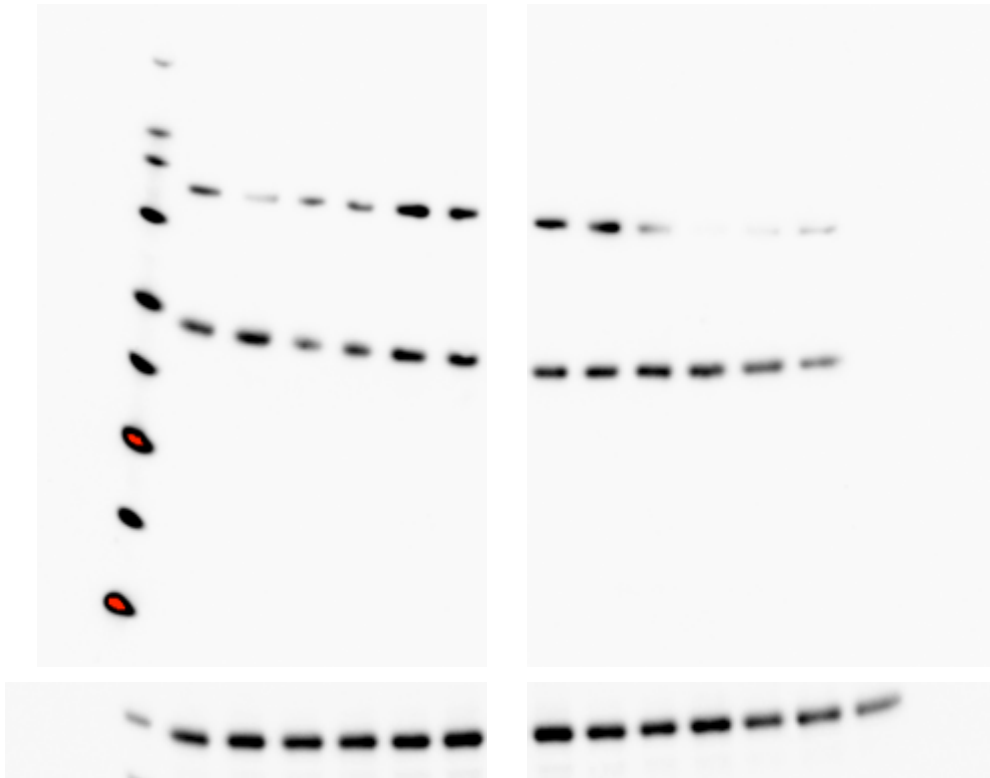
## Figure S18: Phospho-Tyr527-SRC immunoblot results



	P-SRC527	GAPDH	Corrected
Ctr. A1	1,00	1,00	1,00
Ctr. A2	1,33	1,32	1,01
Ctr. A3	1,23	1,25	0,99
Y740C 1	1,26	1,19	1,05
Y740C 2	1,42	1,24	1,14
Y740C 3	1,63	1,16	1,40
L610P 1	1,29	1,24	1,04
L610P 2	1,16	1,20	0,96
L610 3	1,43	1,37	1,05
Ctr. B1	0,98	1,03	0,95
Ctr. B2	1,07	1,41	0,76
Ctr. B3	0,76	1,24	0,61

Immunoblot analysis of fibroblasts harboring the p.(Leu610Pro) and the p.(Tyr740Cys) substitutions. Similar levels of phospho-Tyr527-SRC were present. Results from 3 parallel experiments.

## Figure S19: Tyr527-SRC immunoblot results

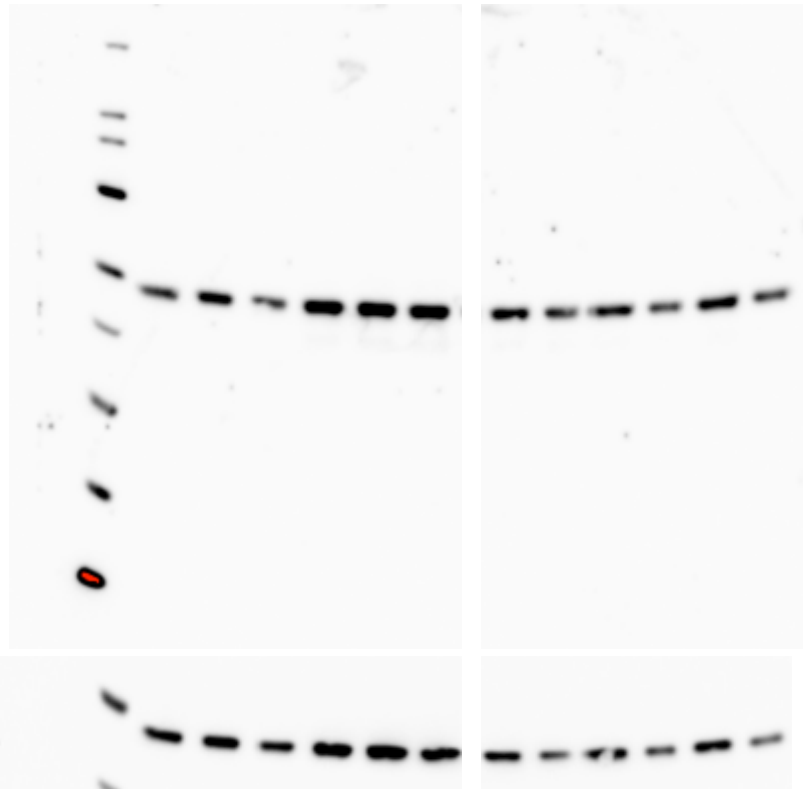


	SRC527	GAPDH	Corrected
Ctr. A1	1,00	1,00	1,00
Ctr. A2	1,38	0,94	1,47
Ctr. A3	0,55	0,50	1,10
Y740C 1	0,75	0,58	1,29
Y740C 2	1,37	0,73	1,89
Y740C 3	1,13	0,48	2,34
L610P 1	1,11	0,55	2,04
L610P 2	1,07	0,59	1,83
L610 3	1,21	0,65	1,85
Ctr. B1	1,16	0,62	1,88
Ctr. B2	1,01	0,77	1,31
Ctr. B3	0,47	0,63	0,75

GAPDH

Immunoblot analysis of fibroblasts harboring the p.(Leu610Pro) and the p.(Tyr740Cys) substitutions. Similar levels of Tyr527-SRC were present. Results from 3 parallel experiments.

**Figure S20:** SRC immunoblot results

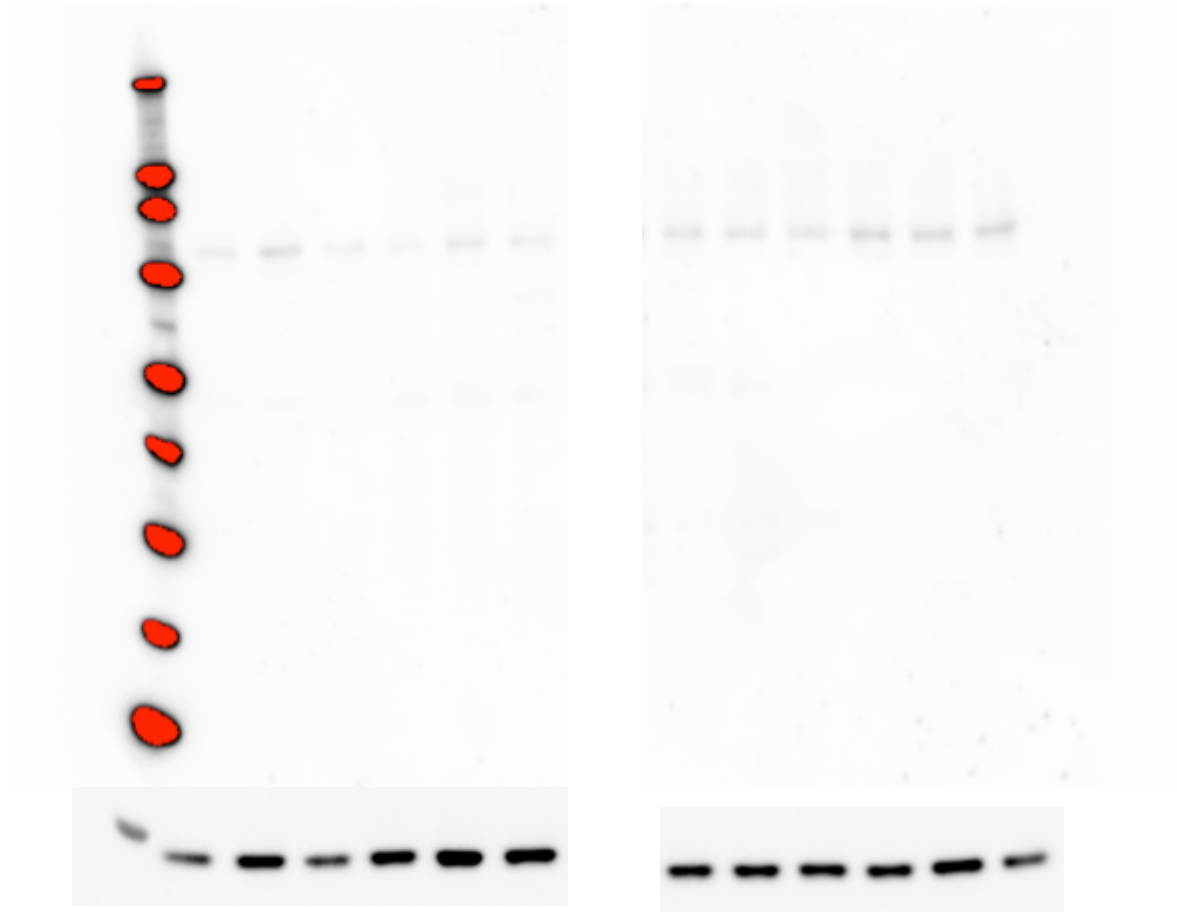


	Total SRC	GAPDH	Corrected
Ctr. A1	1,00	1,00	1,00
Ctr. A2	1,33	1,17	1,14
Ctr. A3	0,75	0,76	0,98
Y740C 1	2,24	1,70	1,32
Y740C 2	2,55	1,96	1,30
Y740C 3	2,39	1,39	1,72
L610P 1	1,39	0,83	1,67
L610P 2	0,93	0,47	1,97
L610 3	1,28	0,76	1,68
Ctr. B1	0,77	0,48	1,60
Ctr. B2	1,49	0,90	1,65
Ctr. B3	0,89	0,43	2,05

GAPDH

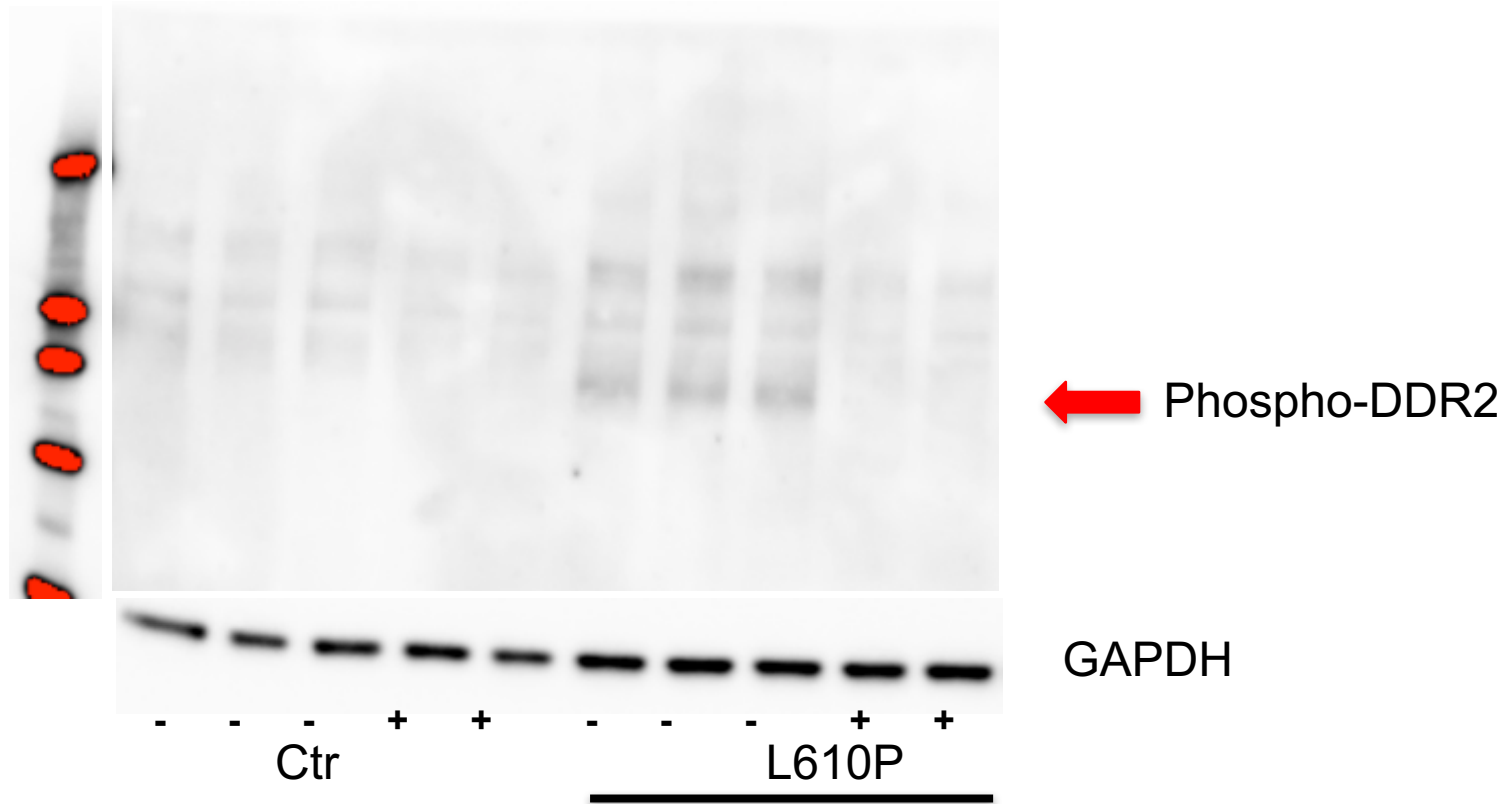
Immunoblot analysis of fibroblasts harboring the p.(Leu610Pro) and the p.(Tyr740Cys) substitutions. Similar levels of total SRC was present. Results from 3 parallel experiments.

## Figure S21: Phospho-STAT1 immunoblot results



Immunoblot analysis of fibroblasts harboring the p.(Leu610Pro) and the p.(Tyr740Cys) substitutions. Similar levels of total Phospho-STAT1 was present. Bands were not measured due to low intensity. Results from 3 parallel experiments.

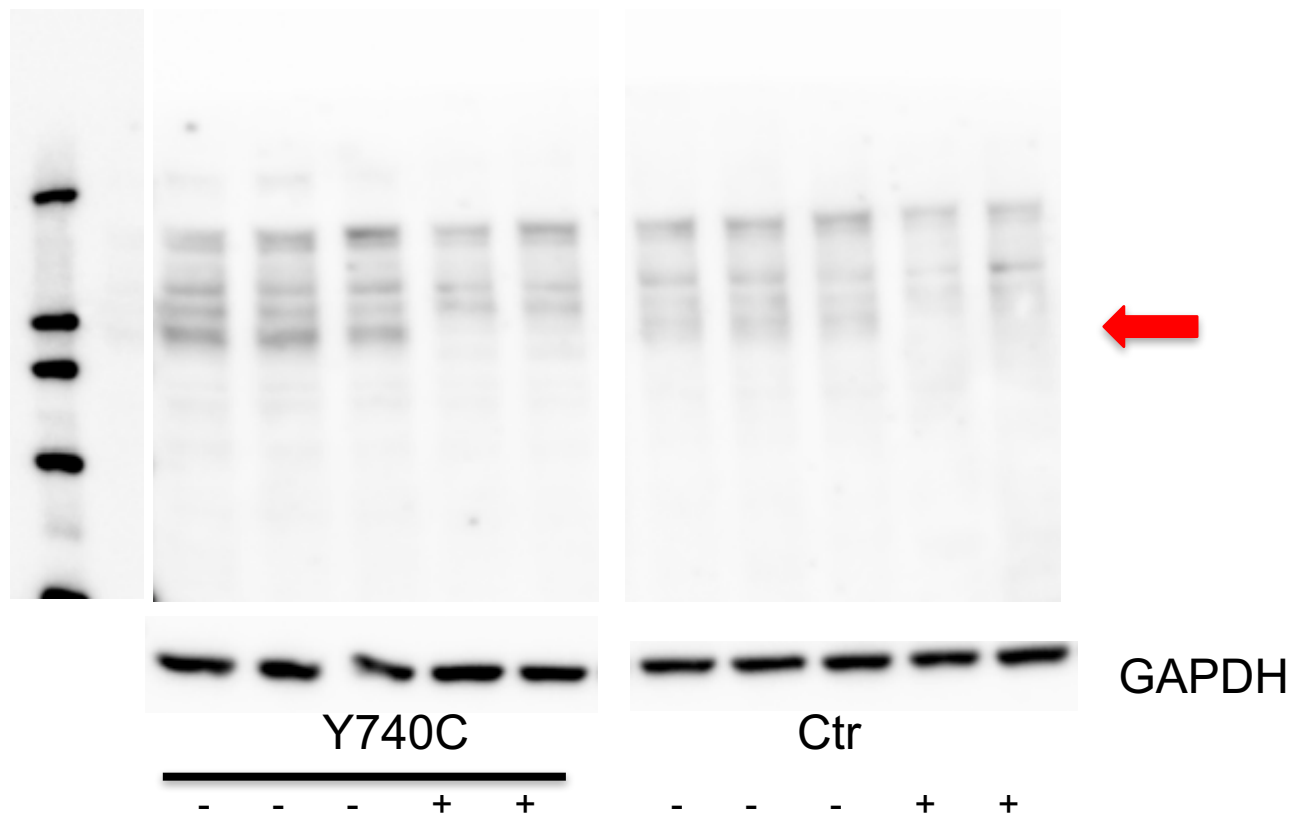
## Figure S22: Phospho-DDR2 immunoblot results after dasatinib treatment



Immunoblot analysis of fibroblasts harboring the p.(Leu610Pro) substitution.

Cells serum-starved overnight were left untreated (-) or treated (+) with 0.1  $\mu$ M dasatinib and harvested for immunoblot analysis after 6 hours. In treated fibroblasts with the p.(Leu610Pro) substitution, the band representing phospho-DDR2 (marked with a red arrow) disappears.

## Figure S23: Phospho-DDR2 immunoblot results after dasatinib treatment



Immunoblot analysis of fibroblasts harboring the p.(Tyr740Cys) substitution.

Cells serum-starved overnight were left untreated (-) or treated (+) with 0.1  $\mu$ M dasatinib and harvested for immunoblot analysis after 6 hours. In treated fibroblasts with the p.(Leu610Pro) substitution, the band representing phospho-DDR2 (marked with a red arrow) disappears.



**Table S1: Overview of phenotypic features**

	<b>Indiv. 1 (age 57 y)</b> <b>Warburg et al.</b> <b>p.(Leu610Pro)</b>	<b>Indiv. 2 (age 58 y)</b> <b>Cinotti et al.</b> <b>p.(Tyr740Cys)</b>	<b>Indiv. 3 (age 31 y)</b> <b>Index mother</b> <b>p.(Tyr740Cys)</b>	<b>Indiv. 4 (age 8 y)</b> <b>Child of indiv. 3</b> <b>p.(Tyr740Cys)</b>	<b>Indiv. 5 (age 3 y)</b> <b>Child of indiv. 3</b> <b>p.(Tyr740Cys)</b>	<b>Indiv. 6 (age 35 y)</b> <b>Singleton indiv.</b> <b>p.(Leu610Pro)</b>
<b>Palpebral fissures</b>	Narrow	Narrow	Normal	Narrow	-	Narrow
<b>Cornea</b>	BE: Advanced corneal vascularization	BE: Advanced corneal vascularization	RE: Advanced corneal vascularization	BE: Superior corneal vascular pannus	BE: Superior corneal vascular pannus	No abnormalities reported
<b>Retina</b>	Retinal dystrophy	Normal fundus	Normal fundus	-	-	-
<b>Vision</b>	BE: 2/60 - Light perception	RE: Light perception LE: 2-3/50	RE: Hand movement LE: 20/16	Normal	-	-
<b>Facial features</b>	Thin nose with small alae nasi Long face, small chin	Thin nose with small alae nasi	Thin nose Long face	Thin nose Long face	Thin nose Long face	Thin nose with small alae nasi
<b>Oral cavity</b>	High palate Abnormal teeth	Gingival hypertrophy Dental prostheses	Normal	-	-	High palate Dental crowding
<b>Ears</b>	Post. rotated ears Ear canal atresia Cholesteatoma Conduct. hearing loss	Post. rotated ears Normal hearing	Post. rotated ears Thin cartilage	Cholesteatoma Thin cartilage	-	Conductive hearing loss
<b>Skin</b>	Thin skin with little subcutaneous tissue	Hyperkeratotic, verrucoid and skin with multiple pigmented keloids	Thin skin with little subcutaneous tissue Linear keloid-like plaques Follicular hyperkeratosis	Thin skin with little subcutaneous tissue Papular rash on arms	Follicular hyperkeratosis	Thin skin with little subcutaneous tissue Angiodermatofibromas Lichenoid lesions Thick keloid-like scars
<b>Joints</b>	Contractures in hands and elbows Kyphosis	Contractures of phalanges, wrists and ankles	Contractures of phalanges and wrists Joint swellings	Contractures of phalanges Joint swellings	Contractures of phalanges Joint swellings	Contractures of phalanges Joint swellings
<b>Hands and feet</b>	Acro-osteolysis Chronic toe ulcers Loss of toenails	Acro-osteolysis Palmar fibrotic bands Loss of toenails	Acro-osteolysis Loss of toenails and toes Cutaneous fusions Sterile abscesses	Palmar fibrotic bands Bluish skin tumor on left foot sole	-	Chronic toe ulcers Loss of toes and forefoot tissue
<b>Miscellaneous</b>	Pneumothorax Hypogonadism Dysphagia	Gynecomastia Mitral valve insuff.	Hypothyroidism Large frontal sinuses	-	-	Pneumothorax Hypothyroidism Mitral valve insuff. Brain infarction Pyloric stenosis Chronic diverticulitis

Indiv. = individual, insuff. = insufficiency, BE = both eyes, RE = right eye, LE = left eye

## Supplemental Methods

### Exome sequencing of individuals 1, 2 and 6

For individuals 1 and 2, DNA was extracted from EDTA whole blood using QiaSymphony (Qiagen, Hilden, Germany). The DNA quality and quantity were evaluated with 1% SeaKem gel electrophoresis and NanoDrop spectroscopy (Thermo Fisher Scientific, Waltham, MA, USA), respectively. Library preparation for exome sequencing was performed using the NimbleGen SeqCap EZ MedExome Target Enrichment Kit (Roche Sequencing, Pleasanton, CA, cat.# 7676581001) and Kapa hyper Prep kit (Roche Sequencing, cat.# KK8504), according to the manufacturers recommendations. Eight individual samples were pooled and then paired-end sequenced on Illumina NextSeq500 using the NextSeq 500/550 v2 sequencing reagent kits (Illumina, San Diego, CA, cat.# FC-404-2002). Demultiplexing (bcl2fastq2-v2.16.0.10), trimming (Trimmomatic-0.33), alignment (bwa-0.7.12), realignment and variant calling (picard-tools-1.129 and GenomeAnalysisTK-3.3-0),<sup>1</sup> were performed in our default diagnostic pipeline, following the Broad recommended best practice guidelines.<sup>2</sup>

Filtering and variant annotation of these data were performed individually in Cartagenia Bench NGS module (Agilent Technologies, Santa Clara, CA), following our routine diagnostic procedure. In short, this involves two separate, but parallel branches of filtration depending on autosomal recessive or autosomal dominant inheritance. In the recessive branch, common variants with a frequency of  $\geq 2\%$  are filtered, while in the dominant branch common variants with a frequency of  $\geq 0,1\%$  are filtered. The source of common variants consisted of 1000 Genomes Phase 1 release v3.20101123, 1000 Genomes Phase 3 release v5.20130502, NCBI ClinVar 20151102, dbSNP build 137 (verified only), ESP6500, ExAC release 0.3 and our own in-house generated variant frequency database based on exome sequencing of 800 individuals. Each source of common variants was queried individually.

Finally, we compared the variant lists of individuals 1 and 2, and made a list of all variants shared by these unrelated individuals. We then removed all variants previously classified as benign in our diagnostic pipeline, and all variants present in dbSNP build 137. Only four heterozygous missense variants remained, and they were in just two genes, *DDR2* and *MUC4*:

- 1) *DDR2*(NM\_001014796.1) c.1829T>C, p.(Leu610Pro), and c.2219A>G, p.(Tyr740Cys).
- 2) *MUC4*(NM\_018406.6) c.7571G>A, p.(Gly2524Asp), and c.14839G>A, p.(Ala4947Thr).

Both *DDR2* variants affected conserved nucleotides and amino acids, and both were

predicted to be detrimental by the following *in silico* prediction programs: PolyPhen2, MutationTester, SIFT and LRT. The CADD score (University of Washington, Hudson-Alpha Institute for Biotechnology, and Berlin Institute of Health) strongly suggested that both variants were unlikely chance findings, being 4.18 (raw score) and 30 (PHRED score) for p.(Leu610Pro), and 4.19 (raw score) and 31 (PHRED score) for p.(Tyr740Thr). In contrast, the two *MUC4* variants were located in non-conserved nucleotides and amino acids, and both were predicted to be benign/neutral or polymorphisms by the *in silico* tools mentioned above. Later, exome sequencing was also done in individual 6, and the same p.(Leu610Pro) variant was found as in individual 1. All variants were verified by Sanger sequencing.

### **Exome sequencing of individuals 3-5**

Solution-hybridization exome capture was performed with the Nimblegen SeqCap EZ Library + UTR (Nimblegen/Roche Sequencing, Pleasanton, CA, USA), and exome sequencing was performed with the HiSeq 2500 sequencer (Illumina). Image analyses and base calling were performed using RTA 1.18.64 and Casava 1.8.2. Reads were aligned to the NCBI Genome browser reference genome GRCh37, hg19 with Novoalign (Novocraft Technologies, Selangor, Malaysia). Samples were sequenced to sufficient coverage such that at least 85% of the targeted exome was called with high-quality variant detection (reported as genotype at every callable position). Genotypes were called with only those sequence bases with Phred base qualities of at least Q20 via Most Probable Genotype<sup>3</sup> (MPG) and an MPG score of  $\geq 10$ .

Patient 3 had three rare heretozygous *de novo* variants (*DDR2*, *TOM1*, *CNTRL*), but the only variant that segregated with the disease and was absent from population databases was the p.(Tyr740Cys) *DDR2* variant. This variant was inherited by two of her three children, patients 4 and 5.

### **ELISA analysis**

Fibroblasts from patients 1 and 3, carrying the p.(Leu610Pro) and p.(Tyr740Cys) variant respectively, and control fibroblasts were obtained and cultured in Dulbecco's modified Eagles' medium (DMEM) - high glucose (Lonza, Verviers, Belgium) supplemented with 10% fetal calf serum, penicillin/streptomycin and glutamine. When 80% confluent, new medium was added and the cells were harvested the following day in 1% NP-40 alternative, 20 mM Tris (pH 8.0), 137 mM NaCl, 10% Glycerol, 2 mM EDTA, 1 mM activated sodium orthovanadate, 10  $\mu$ g/ml aprotinin and 10  $\mu$ g/mL leupeptin. To measure phosphorylated DDR2, a DuoSet IC phospho-DDR2 kit was used (R&D Systems, Oxon, UK, cat.# DYC6170,) following the manufacturer's recommendations. A capture antibody that is specific for human DDR2 binds both phosphorylated and unphosphorylated DDR2 in this sandwich

ELISA. After washing, a HRP conjugated phosphorylated tyrosine antibody is used to detect only the phosphorylated receptor.

### **Western blot analysis**

For Western blot analysis, cells were serum starved over-night, then lysed in 50 mM Tris-HCl, pH 7.5, containing 200 mM NaCl, 5 mM EDTA, 1% Igepal, 1 mM phenylmethylsulfonyl fluoride, complete protease inhibitor cocktail (Roche Diagnostics GmbH, Mannheim, Germany), 0.5% Tween, and 0.1 % SDS. Proteins were separated with a high-resolution gel system (4-12% NuPAGE Novex Bis-Tris Gel; Life technologies, Carlsbad, CA), transferred to nitrocellulose membranes (Bio-Rad, Hercules, CA) and incubated overnight at 4°C with antibodies, as described below at recommended dilutions. The membranes were washed and incubated with horseradish peroxidase-conjugated secondary antibodies from Cell Signaling Technology: anti-rabbit IgG (cat.#7074) and anti-mouse IgG (cat.#7076) for 1 hour at room temperature. Proteins were visualized using the Super Signal West Pico system alone or with added Super Signal West Femto Maximum Sensitivity Substrate (Thermo Fisher Scientific, Rockford, IL). A protein standard (MagicMark; Thermo Fisher Scientific) was used as a molecular weight marker. Chemiluminescence was detected using the ChemiDoc Touch Imaging System (Biorad). To control for equal loading the membranes were blocked again and incubated overnight with anti-GAPDH primary antibody (cat.#G99545-Sigma-Aldrich, St. Louis, MO) and visualized as described above. HEK293 cells transiently transfected with DDR2 vector pMMLV[Exp]-hDDR2[NM\_001014796.1]: IRES:Puro (VectorBuilder, Santa Clara, CA) was used as a positive control for phospho-DDR2 and total DDR2.

#### Antibodies and conditions:

Phospho-Tyr740DDR2 (cat.# MAB25382) and DDR2 (cat.#MAB2538) (R&D systems)

Concentration: 1/1000

Block: 5% Nonfat dry milk in Tris Buffered Saline with 0.1%Tween (TBST)

Short wash in TBST

Primary antibody: 1% Nonfat dry milk in TBST overnight

Wash 10 minutes with TBST x 3

Secondary antibody: 5% Nonfat dry milk in TBST

Was 10 minutes with TBST x 3

Phospho-Tyr542-PTPN11/SHP-2 (cat.#3751), PTPN11/SHP-2 (cat.#3397), phospho-Ser473-AKT (cat.#4060), AKT (cat.#4691), phospho-Thr202/Tyr204-MAPK3/ERK1 (cat.#4370), MAPK3/ERK1 (cat.#4695), phospho-Tyr416-SRC (cat.#69439), Tyr416-SRC (cat.#2102), phospho-Tyr527-SRC (cat.#2105), Tyr527-SRC (cat.#2107), SRC (cat.#2123), phospho-Tyr70-STAT1 (cat.#7649)

Concentration: 1/1000

Block: 5% Nonfat dry milk, 1% BSA, 1% Glycine in Phosphate Buffered Saline with 0.5% Tween (PBST)

Primary antibody: 1% Nonfat dry milk, 1% BSA, 1% Glycine in PBST overnight  
Wash 15 minutes with PBST x 3

Secondary antibody: 1% Nonfat dry milk in PBST  
Was 15 minutes with PBS x 3

Phospho-Tyr580-PTPN11/SHP-2 (cat.#3703)

Concentration: 1/1000

Block: 5% Nonfat dry milk in Tris Buffered Saline with 0.1% Tween (TBST)

Wash 5 minutes with TBST x2

Primary antibody: 5% BSA in TBST overnight

Wash 5 minutes with TBST x 3

Secondary antibody: 5% Nonfat dry milk in TBST

Wash 5 minutes with TBST x 3

### **ClinVar registration**

Both DDR2 variants have been registered in NCBI's ClinVar database:

p.(Leu610Pro) under submission number SUB4623779

p.(Tyr740Cys) under submission number SUB4624426

### **References**

1. McKenna A, Hanna M, Banks E, et al. The Genome Analysis Toolkit: a MapReduce framework for analyzing next-generation DNA sequencing data. *Genome Res* 2010;20:1297-303.
2. Van der Auwera GA, Carneiro MO, Hartl C, et al. From FastQ data to high confidence variant calls: the Genome Analysis Toolkit best practices pipeline. *Curr Protoc Bioinformatics* 2013;43:11 10 1-33.
3. Johnston JJ, Sanchez-Contreras MY, Keppler-Noreuil KM, et al. A Point Mutation in PDGFRB Causes Autosomal-Dominant Penttinen Syndrome. *Am J Hum Genet* 2015;97:465-74.